Influence of Prolonging Vulcanization on the Structure and Properties of Hard Rubber

Ya Wang,[1] Yiqing Wang,[1] Ming Tian,[1] Liqun Zhang,[1] Jun Ma[2]

[1]*The Key Laboratory of Beijing City on Preparation and Processing of Novel Polymer Materials, Beijing University of Chemical Technology, 100029*
[2]*School of Advanced Manufacturing and Mechanical Engineering, The University of South Australia, Adelaide, South Australia, 5095*

Received 19 September 2005; accepted 4 February 2007
DOI 10.1002/app.27086
Published online 20 September 2007 in Wiley InterScience (www.interscience.wiley.com).

ABSTRACT: This research on vulcanization illuminates the structure–property relationship of hard rubber with prolonging vulcanization. At the early stage of curing, polysulfur reacts with styrene–butadiene rubber (SBR) macromolecules to form chemical crosslink, as evidenced by the significant increase of modulus during vulcanization. The chemical crosslink is followed by a large amount of interchain attraction, which is due to the modification of SBR macromolecules by combined sulfur. The combined sulfur is formed by the reaction of sulfur atom with SBR backbone, which improves the polarity of SBR macromolecules since sulfur is polar. The influences of chemical crosslink and interchain attraction on the mechanical properties, thermal properties, dynamic mechanical properties, and fracture morphology were analyzed. © 2007 Wiley Periodicals, Inc. J Appl Polym Sci 107: 444–454, 2008

Key words: rubber; vulcanization; morphology; fracture; thermal properties

INTRODUCTION

Hard rubber, also entitled ebonite, is one kind of rubber with glass transition temperature (T_g) higher than room temperature; it is prepared by long-time curing with a much higher content of sulfur than those used in common rubbery products.[1,2] Hard rubber possesses high resistance to chemicals, good electrical insulating properties, excellent strength properties, and the ability to be machined easily, which leads to wide application across a number of industries.[3,4]

Meltzer studied the influence of fillers and degree of vulcanization on the mechanical properties of hard styrene–butadiene rubber (SBR) – butyl rubber; T_g is found increasing with degree of vulcanization.[5] The author also reported the appropriate ratio of crosslink to sulfur atoms, 0.04–0.07 and 0.10–0.13 in hard rubber for natural and SBRs, respectively.[6,7] For *cis*-polybuadiene rubber, the ratio turns from 0.17 to 0.06 and for *trans*-polybuadiene rubber it turns from 0.15 to 0.07.[8] Church reported the influence of vulcanization temperature on the properties of hard rubber; a number of properties were investigated for small samples of the same materials, which were vulcanized for various time at different temperatures.[9] Bhaumik et al. developed a method to determine the reaction heat during the curing by differential thermal analysis (DSC); heat evolution is observed first with samples containing about 7% sulfur and therefrom the amount of heat evolved shows a nearly linear increase up to 31% sulfur.[10–12] Scott studied the influence of the vulcanization on the properties of hard rubber.[13] It is found that there is an optimum proportion of sulfur, as the yield temperature rises to a maximum and then falls with increasing the sulfur percentage. The author shows that the increase of combined sulfur by prolonging vulcanization is more effective in producing the characteristic properties of hard rubber (e.g., high yield temperature, hardness, and resistance to petroleum) than the quantitive increase of sulfur. Dermody studied the stress–strain curves of the hard rubber.[14]

In spite of the previous intensive investigation into hard rubber in the 1960s, there is no systematic report on the structure–property relationship of hard rubber with prolonging vulcanization with a fixed amount of sulfur. In this study, SBR samples were cured by a fixed amount of sulfur with various curing time. The structure of the cured SBR was analyzed by the curing characteristics and the swelling analysis. The mechanical property, thermal property, and the dynamic mechanical property were investigated and analyzed from the point of structure.

Correspondence to: L. Zhang (zhangliqunghp@yahoo.com) or J. Ma (abcjunma@hotmail.com).

Contract grant sponsor: National Natural Science Foundation of China; contract grant number: 05173003.

TABLE I
The Recipes in This Study

Content (phr)	Basic sample (SBR)	Basic sample (NR)	Sample one	Sample two
SBR	100.0	–	100.0	–
NR	–	100.0	–	100.0
MgO	5.0	–	–	–
ZnO	–	5.0	3.0	5.0
SA	–	2.0	1.0	2.0
Accelerant TT	–	0.2	–	0.2
Accelerant DM	3.0	0.5	–	0.5
Accelerant D	1.5	0.5	–	0.5
Accelerant CZ	–	–	1.2	–
Antioxidant RD	–	–	1.0	–
Antioxidant 4010NA	2.0	–	1.0	–
Sulfur	32.0	30	1.8	1.5
Total amount	143.5	138.2	109.0	109.7

Note: phr means per hundred rubber in weight.

Fracture surfaces of the tensile samples were analyzed by Scanning Electron Microscopy (SEM).

EXPERIMENTAL

Materials

Styrene–butadiene rubber (SBR) (Tradename SBR1502) was available from Jilin petrochemical Corp. (Jilin Province, China) with a weight average molecular weight of 500,000 g/mol and density of 0.9264 g/cm^3; and NR (Tradename SCR5, similar to RSS3) was available from Yunnan Xishuangbanna Dongfeng mill. Insoluble sulfur was offered by Beijing Chemical Corp. Toluene (AP), acetone (AP), and other chemicals were commercially available.

Formulations and vulcanization

The recipes used here are shown in Table I and the accelerators are specified in Table II. Rubber was mixed with additives by a two-roller mill and then the compound was slightly cured at 150°C under the pressure of 15 MPa for 15 min. Finally, it was further cured at 150°C in an oven for 1, 2, 4, and 8 h, respectively.

Characterization

The curing behavior was measured by P3555B2 Disc Rheometer at 150°C. The tensile strength test was conducted at room temperature according to ASTM D2707-1985. Vicat softening temperature (VST) was measured with ISO 306 : 1994.

Dynamic mechanical properties

The dynamic mechanical properties were measured with DMTA IV (USA Rheometric Scientific). The samples were run on tensile mode in nitrogen at 1 Hz over a temperature range of −100°C to 150°C with 5°C/min.

DSC analysis

The samples for DSC analysis were preheated to remove thermal history. The measurement was carried out using 204F1-DSC(NETZSCH), equipped with a liquid nitrogen-cooling device, with a temperature range of −60°C to 140°C at a heating rate of 10°C/min.

Swelling studies

The swelling ratio $W\%$ (wt %) was measured by the method of equilibrium swelling. The samples were swelled in toluene at 23°C until equilibrium, during which uncombined sulfur was dissolved in toluene. Then the samples were immerged in acetone to remove the extracted sulfur, followed by drying in a highly degassed vacuum oven at for 24 h at 80°C. The weight of the samples before dipped is named as W_1; when the immersed samples achieved equilibrium, the samples were weighted as W_2. The precision of the weight was 0.0001 g and all values were rounded for four significant numbers. After dried by vacuum, the samples were weighted as W_3. The swelling ratios were determined by the following eq. (1).

$$W\% = (W_2 - W_1)/W_1 \quad (1)$$

The weight percentage of the consumed sulfur ($W_s\%$) can be obtained by the following eq. (2).

$$W_s\ \% = 1 - (W_1 - W_3)/(S\% \times W_1) \quad (2)$$

where S%, defined as the sulfur contents in the rubber samples, is equal to 0.223 (which means 32 phr sulfur in 100 phr SBR) by weight; the $(W_1 - W_3)$ represents the unconsumed sulfur, which is dissolved in the solvent.

TABLE II
Chemical Compositions of Material and Additive Used in This Study

Material and additive	Chemical composition
SBR	Butylbenzene rubber
Accelerant DM	2,2′-dibenzothiazole disulfide
Accelerant D	Diphenylguanidine
Accelerant CZ	*N*-cyclohexyl-2-benzothiazole sulfenamide
Accelerant TT	Tetramethyl thiuram disulfide
Antioxidant 4010NA	*N*-isopropyl-*N*′-phenylenediamine
Antioxidant RD	Polymerized-2,2,4-trimethyl-1, 2-dihydroquinoline
SA	Stearic acid

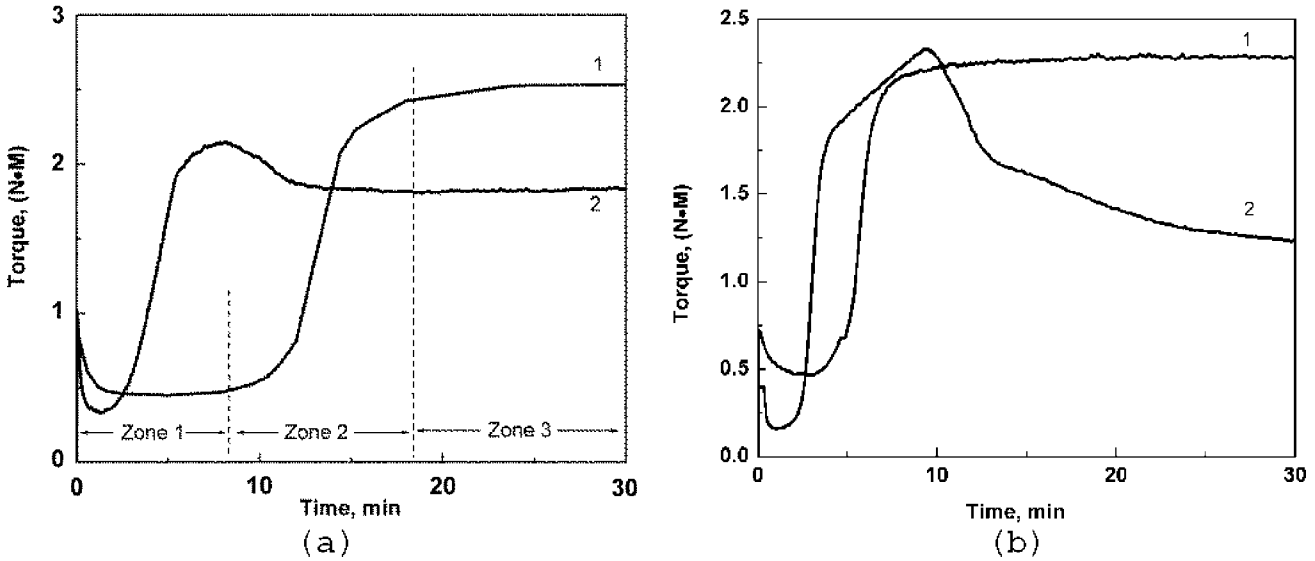

Figure 1 (a) Torque versus time curves of soft SBR (with 1.8 phr sulfur) and hard SBR (with 32 phr sulfur) for Curve 1 and Curve 2, respectively; (b) Torque versus time curves of soft NR (with 1.5 phr sulfur) and hard NR (with 32 phr sulfur) for Curve 1 and Curve 2, respectively.

SEM

Fracture surfaces of tensile samples were prepared at room temperature and examined with a thin gold coating. Micrographs were obtained at magnification from 20 to 3000 using S-2501 SEM.

RESULTS AND DISCUSSION

Vulcanization characteristics

During vulcanization, heat evolution is observed first with samples containing about 7% sulfur and therefrom the amount of heat evolved shows a nearly linear increase up to 31% sulfur.[11,12] Hence, we chose the amount of 32.0 phr sulfur for 100 phr SBR—such a high concentration can ensure a high crosslink density. As shown in Figure 1(a), curing time was chosen for each sample according to its sulfur amount so that each sample reached T90% of the rheometer curve. However, the curing pattern of the hard rubber (Curve 2) is completely different to Curve 1. Zone 1 is obviously shortened from 8 min for the Curve 1 to 1 min for the Curve 2; this is explained as that more sulfur promotes higher degrees of vulcanization, making it occur earlier. For the same reason, Zone 2 is shortened to 7 min from 16 min for the curve 1. In Zone 3, the maximum torque for the curve 1 is 2.5 Nm, 19% higher than that for the Curve 2 for SBR containing much more sulfur, indicating a higher crosslink density at the curing temperature for SBR containing much less sulfur. This in contradiction to what we expected—higher sulfur content for hard rubber should produce higher crosslink density than common elastomer containing much less sulfur. This experiment was repeated twice and each time the same result was obtained. We also cured natural rubber with 1.5 phr and 32.0 phr sulfur and the torque-curing curves are shown in Figure 1(b). Similarly, the modulus at the curing temperature reaches maximum and then drops down obviously with high concentration sulfur. There must be some particular reasons for this.

It is well known that there are two types of sulfur existing in the process of vulcanization, i.e., free sulfur and combined sulfur. According to Scott's research,[15] the amount of the free sulfur decreases with vulcanization, since it reacts with the rubber backbone and forms a number of combined sulfur, including sulfur ring, polysulphide, monosulphide, and disulphides. Of which, Sulfur ring (such as methylthiacyclopentane) and polysulphide were reported as main types.[1,13]

When the curing proceeded, polysulfide reacted with SBR to form chemical crosslink; that is, more chemical bonds between rubber macromolecules were formed. On the other hand, the formation of the combined sulfur improved the interchain attraction of the rubber macromolecules, since sulfur is fairly polar and the ring can combine with the macromolecules, as shown in Figure 2. In conclusion, there are two types of molecular interaction that occurred during the formation of networks: the chemical crosslink produced by the chemical bond between sulfur and rubber macromolecule, and the interchain attraction provided by the polar interaction between the modified rubber macromolecules. While the chemical crosslink does not change when

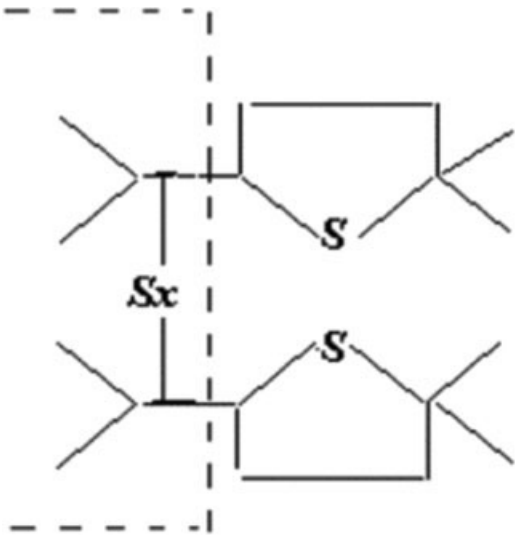

Figure 2 Schematic representation of sulfur combined with SBR.

heated below thermal degrading temperature, the interchain attraction decreases when heated and may vanish at high temperature.

On the basis of the above analysis, the two contradictive trends occurred in Figure 1 are explained as follows. The total chain interaction produced in the formation of network increases, because sulfur reacts with SBR. On the other hand, however, the unsaturated SBR macromolecules thermally degrade in the process of curing at 150°C. The degradation will be more severe if the additives used contain polar groups. SBR with 32.0 phr sulfur shows lower modulus at the curing temperature in Figure 1 for two reasons. One is that the interchain attraction, caused by the modified SBR macromolecules by the combined sulfur, decreases and may disappear at 150°C (this will be confirmed in Fig. 5). On the other hand, the excessive polar sulfide promotes the degradation of the macromolecules, which reduces the total chain interaction more severely than the benefit of the chemical crosslink density produced by polysulfide. Therefore, Figure 1 shows only the trend of the chemical crosslink during vulcanization. It increases tremendously during the early period of curing and then reaches a plateau; since then it decreases slightly due to the gradually disappeared interchain attraction.

Swelling analysis

Figure 3(a) reflects the consumption of sulfur and the swelling ratio of the cured SBR with proceeding vulcanization. The detailed data are shown in Table III. Two characteristic zones are found for the consumption of sulfur. Zone 1 and Zone 2 are initiated from 1 to 4 h and 4–8 h, respectively. The amount of sulfur is linearly consumed in Zone 1 and therefrom the amount remains almost constant. This means that most of the sulfur is reacted with SBR in zone 1; that is, the chemical crosslink density increases tremendously at the earlier stage of vulcanization and then remains almost constant. The swelling ratio of the cured SBR indicates the curing degree. In Figure 3, the swelling ratio decreases steadily with prolonging vulcanization and there is no obvious change on the slope; this means that the interactions in the network, including chemical crosslink and interchain attraction, increases steadily during curing. Given the fact that the chemical crosslink density increases tremendously at the earlier stage of vulcanization and then remains almost constant, the increase of the network interaction from 4 to 8 h can be

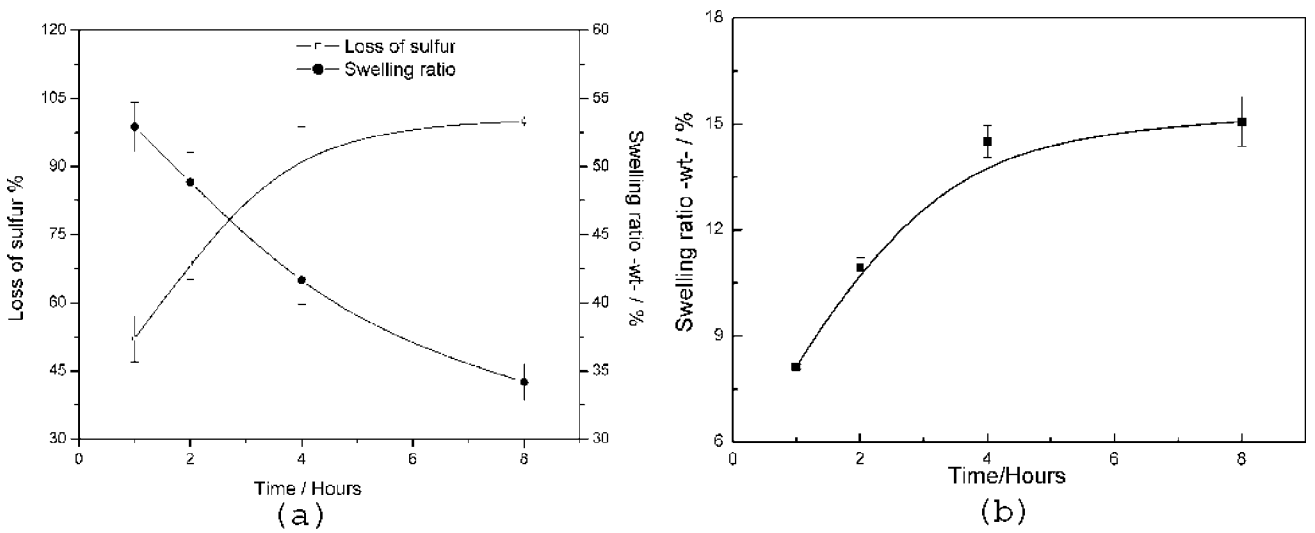

Figure 3 The sulfur loss ratio and SBR swelling property with prolonging vulcanization: (a) At room temperature, (b) At 75°C.

TABLE III
Swelling Data of Vulcanizates with Different Curing Time

Samples	W_1 (g)	W_2 (g)	W_3 (g)	W_s (%)	W (%)
a	0.3978	0.6066	0.3553	52.09	52.89
b	0.3519	0.5238	0.3273	68.65	48.85
c	0.2723	0.3857	0.2706	97.20	41.66
d	0.3265	0.4381	0.4001	$\sim$ 100	34.18

Sample a: 1 h; sample b: 2 h; sample c: 4 h; and sample d: 8 h.

attributed to the increase of interchain attraction, caused by the modification of rubber macromolecules by the combined sulfur.

To confirm the above analysis, a swelling test was conducted in dimethyl sulfoxide at 75°C, higher than the glass transition temperature of the hard rubber. As shown in Figure 3(b), the swelling ratio increases at the temperature with curing time, which is opposite to Figure 3(a) conducted in toluene at room temperature, indicating a very different network interaction at the temperature. Chemical crosslink is well known not to change significantly with temperatures except thermal degradation occurs; in contrast, the interchain attraction decreases with temperature. At the high temperature, hence, interchain attraction decreases or disappears and cannot provide as strong network interaction as that in room temperature. On the other hand, the unsaturated SBR macromolecules experienced thermal degradation during vulcanization. Both factors contributed to the increased swelling ratio. Therefore, the increase of the network interaction in the period from 4 to 8 h can be attributed to the increase of interchain attraction, caused by the modification of rubber macromolecules by the combined sulfur.

In conclusion, the curing mechanism with prolonging vulcanization is generalized as below. Sulfur reacts into polysulfide in the very earlier period of vulcanization as a result of phase separation; this takes 2–10 min, depending on the amount of sulfur. Then the chemical crosslink is formed by the reaction of polysulfide with SBR in the first dozens of min. Afterwards the reaction of polysulfide with SBR mainly produces interchain attraction by forming combined sulfur. The rings modify the SBR macromolecule and improve the interchain attraction. Thermal degradation does occur, but it is not the main trend.

Thermal properties

The glass transition temperatures (T_g) can be treated as the temperature below which chain segments no longer have sufficient energy for rotation and hence wriggling of the molecular chains; it is a finite temperature range through which bond rotation becomes more and more difficult and the deformational response to a stress takes longer and longer.

The thermal properties of SBR with 32.0 phr sulfur cured with different time were investigated by DSC. As shown in Figure 4, T_g of sample (a) and (b) are −9.6°C and 0.9°C, respectively, meaning elasticity at room temperature. The T_g of sample (c) and (d) are 36.3°C and 63.4°C, respectively; this indicates these two samples are in glassy state at room temperature.

With increasing temperature at 0.8°C/min, the deformation of hard rubber cured by 8 h is shown in Figure 5. A sharp increase of deformation was observed from 75 to 82°C; this means the disappearance of the interchain attraction provided by the SBR macromolecules modified by the combined sulfur. It corresponds to Figure 1 and confirms our analysis on the curing mechanism.

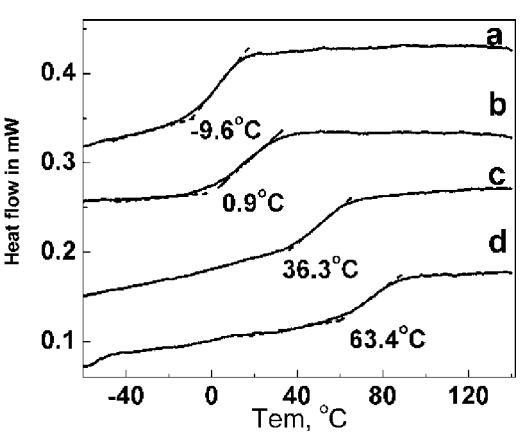

Figure 4 DSC curves of vulcanizates at different vulcanizations time: (a) 1 h; (b) 2 h; (c) 4 h; (d) 8 h.

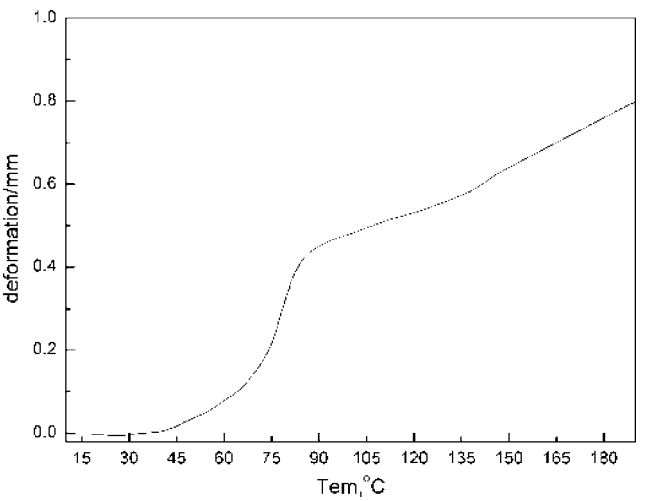

Figure 5 Deformation versus temperature of hard rubber cured with 8 h.

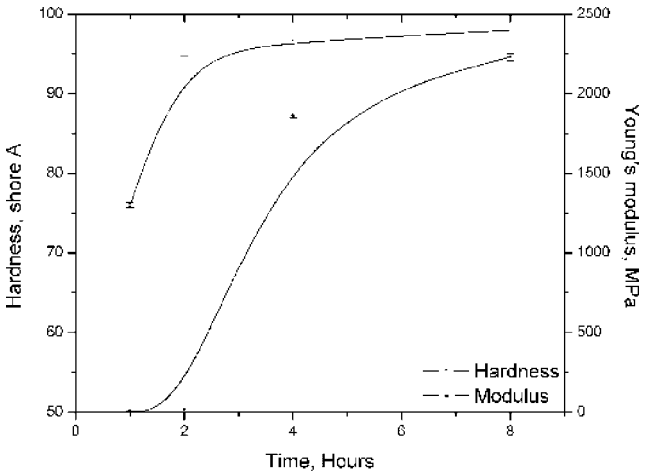

Figure 6 The hardness and Young's modulus with prolonging vulcanization.

The main factors determining the T_g include chain stiffness, interchain attraction, molecular symmetry, copolymerization, branching and crosslinking, solvents and plasticizers[16]; of which, chain stiffness is considered as the most dominating factors. The chemical crosslink is the basic network interaction, which obviously improves the chain stiffness. The interchain attraction, provided by the rubber backbone modified by the combined sulfur, also raises the T_g significantly. But this attraction decreases with temperature and vanishes at high temperature.

Mechanical properties

The mechanical properties of SBR vulcanizates with 32.0 phr sulfur contents cured with different vulcanization time are shown in Figures 6–8 and the detailed data are available in Table IV. The lines in the Figures only show the tendency of the data. The hardness

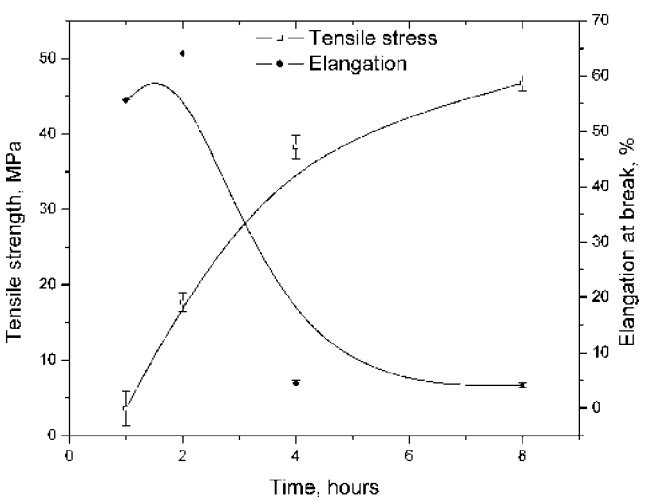

Figure 7 The tensile strength and elongation at break with prolonging vulcanization.

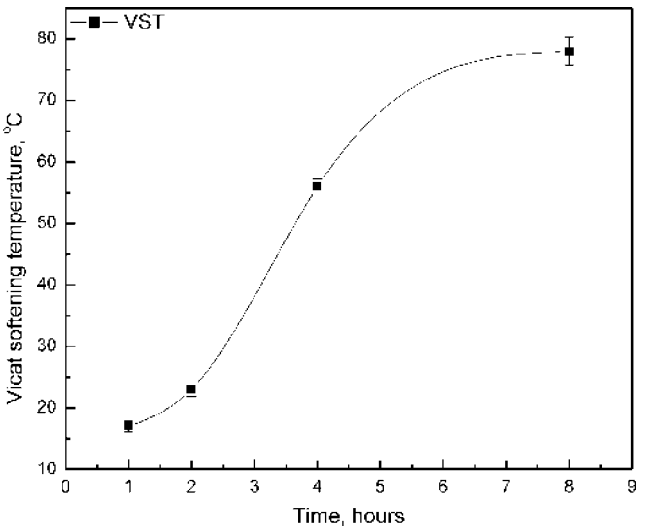

Figure 8 Vicat softening temperature with prolonging vulcanization.

increases significantly in the first 1–2 h and then changes slightly in Figure 6; this means the hardness is mainly dependant on the chemical crosslink of SBR at the early stage of vulcanization. The Young's modulus remains rather low from 1 to 2 h and then increases obviously until 4 h later. Compared with hardness, the Young's modulus keeps low until a certain amount of interchain attraction formed after 2 h curing. The modulus might mainly depend on the interchain attraction, since it changes dramatically from 2 to 4 h.

With prolonging curing, the elongation at break in Figure 7 increases to 64.1% at 2 h and then decreases. It reaches 4.5% at 4 h and then remains almost constant, indicating such a curing time might be ideal for hard rubber. From 2 to 4 h, more network interaction forms and this confines the movement of rubber macromolecules. The tensile strength generally increases with vulcanization, meaning it depends on both chemical crosslink and interchain attraction. The improvement of tensile strength from 1 to 4 h is more than that from 4 to 8 h; this shows the enhancement of interchain attraction slows down from 4 to 8 h.

TABLE IV
Mechanical Properties and Thermal Properties of Vulcanizates at Different Curing Time

Samples	Hardness, shore A	Elastic modulus (MPa)	Tensile strength (MPa)	Elongation at break (%)	VST (Celsius)
a	75.8	6	3.62	55.6	17
b	95.0	17	17.68	64.1	23
c	96.5	1861	38.28	4.5	56
d	97.9	2231	46.72	4.1	78

Sample a: 1 h; sample b: 2 h; sample c: 4 h; and sample d: 8 h.

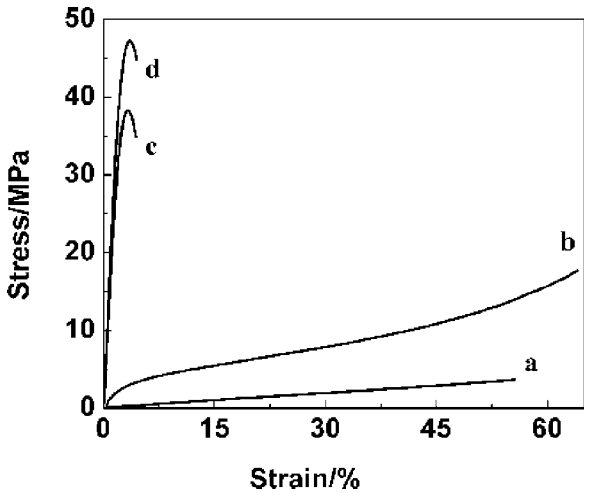

Figure 9 Stress–strain curves of vulcanizates at different curing time: (a) 1 h; (b) 2 h; (c) 4 h; (d) 8 h.

VST is the resistance of materials to heat deformation; it is determined by the ability of macromolecules to wriggle or slip. In Figure 8, the VST improves with vulcanization and reaches a plateau at 7 h. With prolonging vulcanization, more chemical crosslink and interchain attraction occur and this confines the movement of SBR macromolecules. Hence, VST improves with vulcanization.

Stress–strain curves of the SBR vulcanizates with 32.0 phr sulfur contents were given in Figure 9. Samples (a) and (b) show completely different characteristics to sample (c) and (d). Sample (a) and (b) are cured by 1 and 2 h, respectively; both indicate high elongation and low strength due to low network interaction—characteristics of polymer in rubber state; this is mainly provided by chemical crosslink according to our previous analysis. Sample (c) and (d) are cured by 4 and 8 h, respectively; both indicate low elongation and high strength due to high crosslink density—characteristics of polymer in glassy state; this is due to the chemical crosslink and the interchain attraction. On the basis of the above discussion, a conclusion to be made is that the chemical crosslink, formed during the early curing stage, contributes to the rubbery state of the material, indicating the low strength and high elongation at break. However, the interchain attraction, provided by the SBR backbones modified by the combined sulfur, should attribute to the glassy state of the material, indicating the high modulus, high strength, and low elongation at break of hard rubber.

Dynamic mechanical property

The dynamic mechanical properties of SBR with 32.0 phr sulfur cured by different time were shown in Figure 10. With prolonging vulcanization, the peak intensity decreases, but the peak position moves to higher temperature with an increased peak width (measured by the full width at half-maximum). Since higher degree of network interaction occurs during vulcanization, it is understandable that T_g increases and the peak position moves to higher temperature. The decrease of the peak intensity probably means the reduction of the mobility of the network chains, as more crosslinking happens during curing. In previous literatures, broadened peak width was often explained as the increased heterogeneity.[17,18] Here, tan δ represents the molecular mobility of the crosslinked molecular chain; chain lengths between two crosslink points are different each other. Hence, more various chain lengths were formed during vulcanization and this may lead to the broadened tan δ peak. In comparison, SBR with 1.8 phr sulfur shows the lowest T_g, the highest peak position and the smallest peak width. This is due to the much less amount of sulfur, which produces the lowest degree of network interaction. All the observation is in agreement with the conclusion of DSC test that the conversion of rubber form soft to hard state is due to the interchain attraction provided by the modified SBR macromolecules by the combined sulfur.

Fracture morphology of tensile sample

Figure 11 is the SEM microphotographs of fractured tensile sample (a) with 1 h curing. In Figure 11(a) with the lowest magnification, it is discernable that fracture initiated from the right-bottom corner, albeit no obvious feature found. Certain amount of tearing pattern is observed in Figure 11(b,c) with higher magnification. This is typical fracture morphology

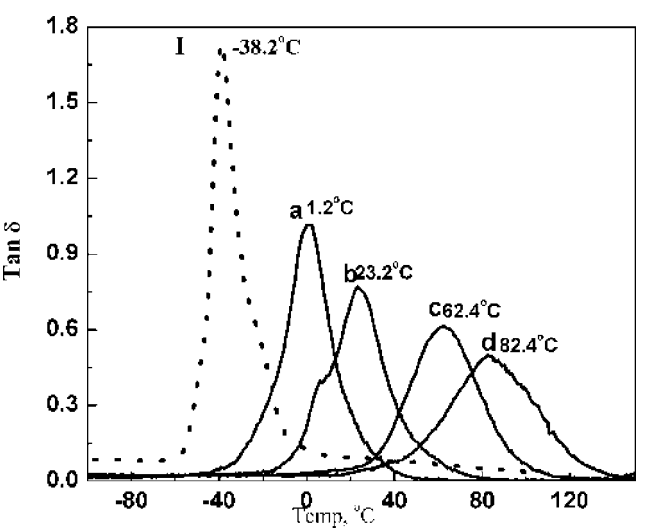

Figure 10 Loss tangent of DMTA spectra of vulcanizates at different vulcanizations time: (a) 1 h; (b) 2 h; (c) 4 h; (d) 8 h; sample I is cured with 1.8 phr sulfur; the position of the loss tangent maximum is labeled.

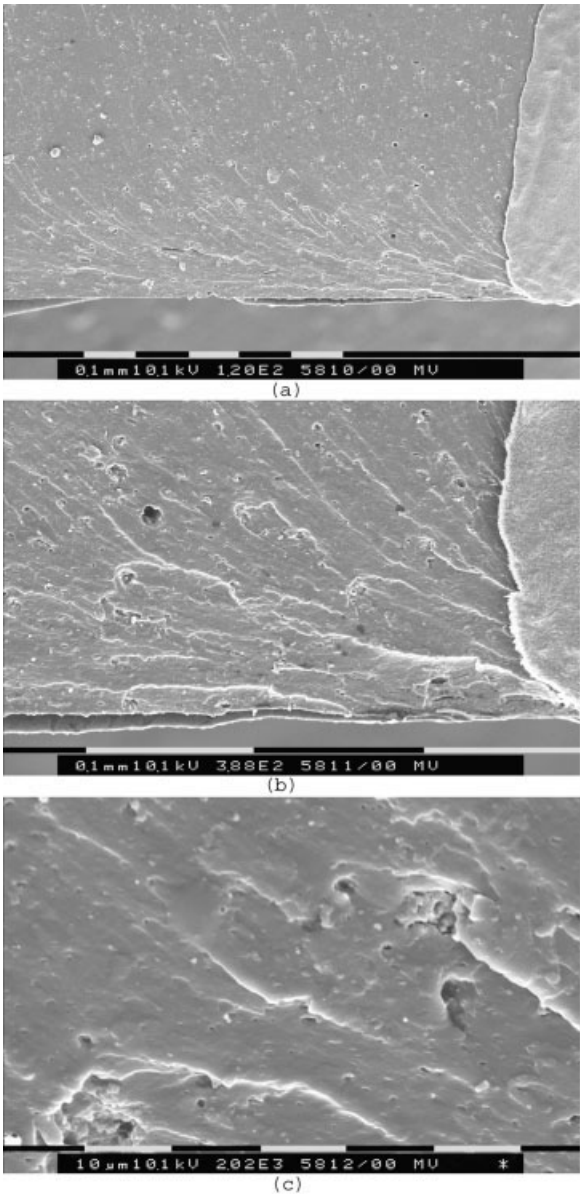

Figure 11 SEM microphotographs of sample (a) with 1 h curing.

for elastic materials.[19,20] When the curing time prolonged to 2 h, scale-like pattern is a universal feature for the fractured tensile sample (b), as shown in Figure 12. The scale-like morphology is similar to those of reinforced elastomers[18,20] meaning, a higher tensile strength for the sample (b) than the sample (a) in Figure 11. This result is in agreement with the preceding analysis on mechanical properties in Table IV.

Microphotographs in Figure 13 are the tensile fracture morphology of sample (c). In Figure 13(a), two characteristic zones are found. On the bottom is the slow propagation zone (Zone 1), above which is the quick propagation zone (Zone 2). Fracture occurs first in Zone 1 and then extends in Zone 2. Details of Zone 1 are revealed in Figure 13(b–d). Many tearing patterns are observed, forming hackle-like feature; there is also a little amount of striation deformation. Details of Zone 2 are shown in Figure 13(e–g). Compared with the morphology of the sample (b) shown in Figure 12, a larger amount of scale-like pattern with higher degree of deformation is found. In general, more obvious deformation was shown on the sample (c) than the sample (b). This means fracture occurs at a higher carrying load compared with the sample (b) which is cured with shorter time, corresponding to the previous mechanical property analysis. This type of two-zone morphology is similar to that of hard epoxy resin, showing its high hardness; this corresponds to the data shown in Table IV.

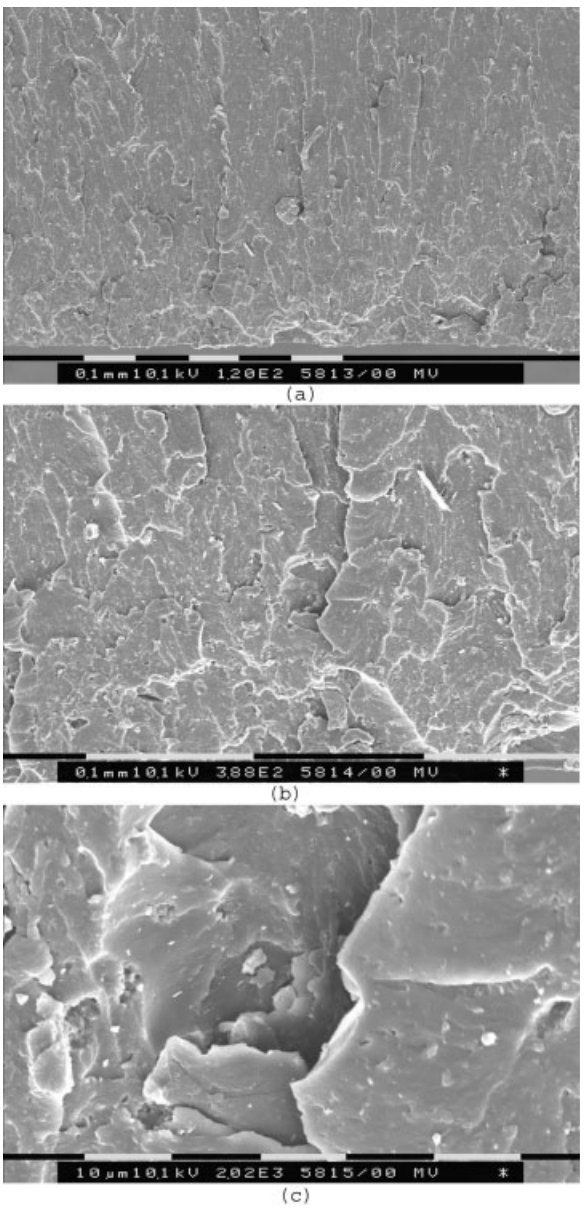

Figure 12 SEM microphotographs of sample (b) with 2 h curing.

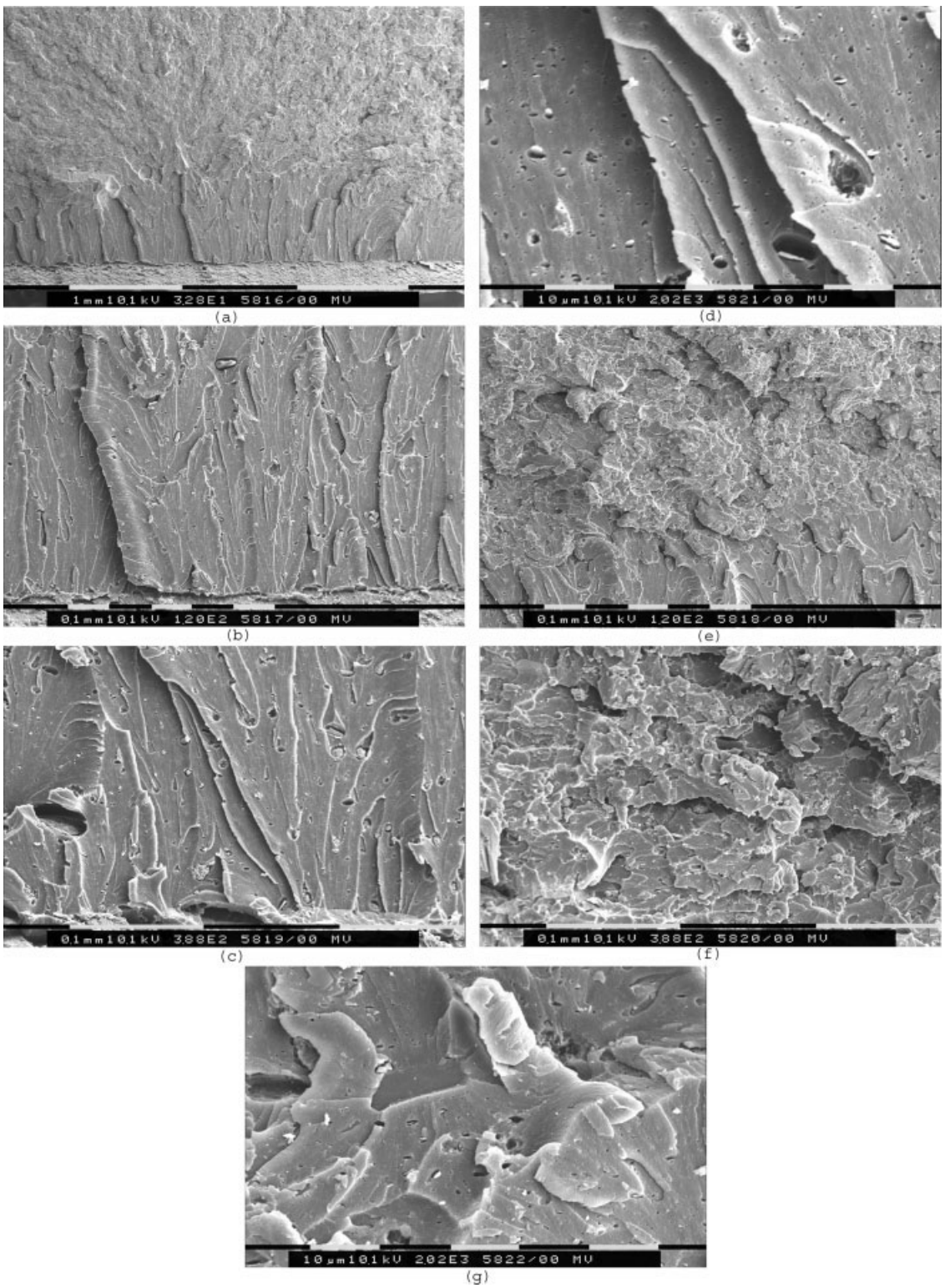

Figure 13 SEM microphotographs of sample (c) with 4 h curing.

When cured 8 h, the sample (d) in Figure 14 shows a similar two-zone morphology to the sample (c). In Figure 14(b–d), however, Zone 1 indicates more striation deformation rather than hackle-like structure. The height of Zone 1 shown in Figure 14(a) also is a little higher than that in Figure 13(a). Less amount of scale-like structure was found in Zone 2 in Figure 14(e–g), in comparison with Zone 2 in Figure 13(e–g). In conclusion, the deformation degree of the tensile-fractured sample (d) is less than sample (c). This is

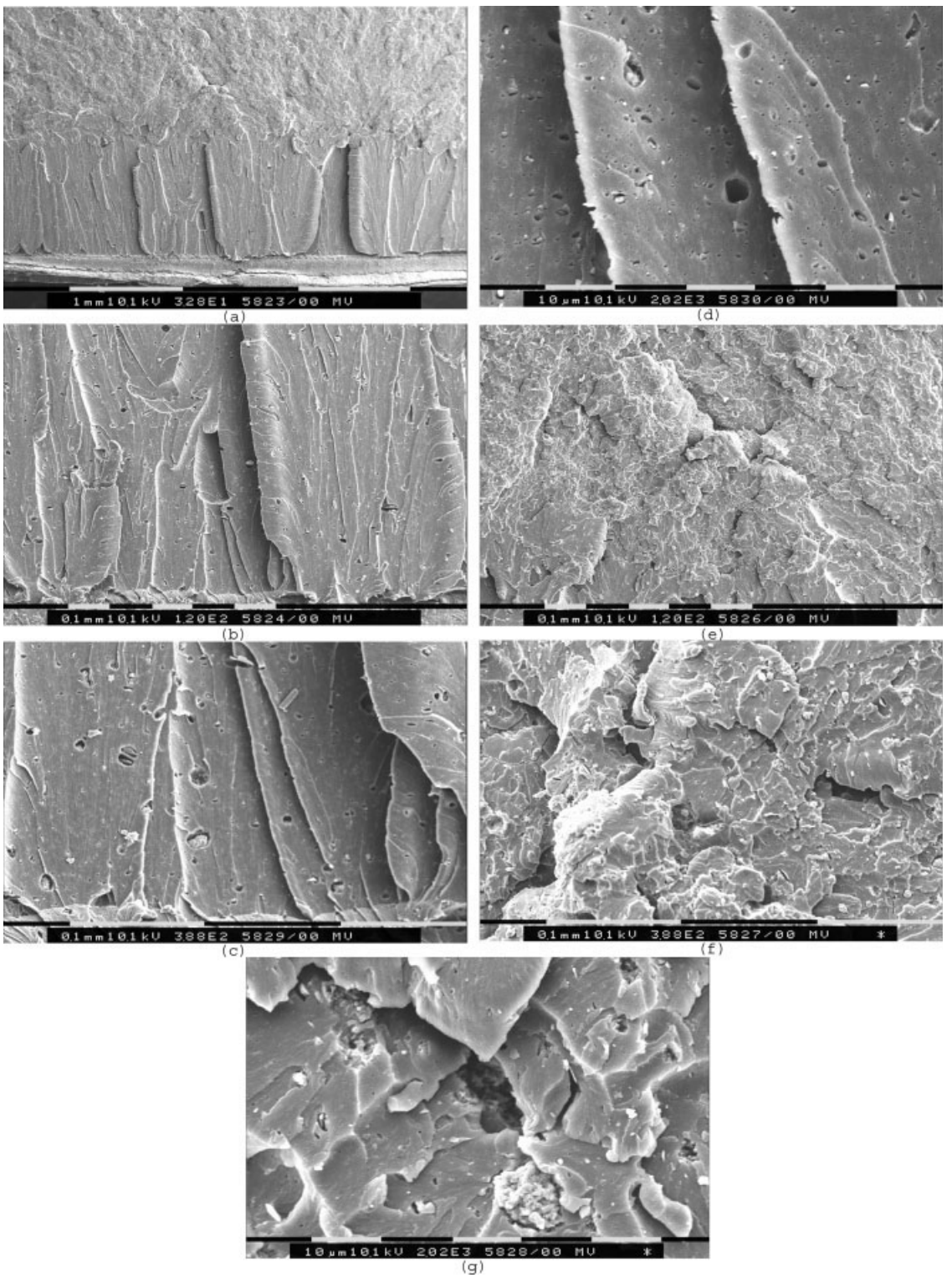

Figure 14 SEM microphotographs of sample (d) with 8 h curing.

caused by the different degree of network interaction with various curing time. According to our previous analysis, chemical crosslink occurs at the early stage of curing; since then the interchain attraction is formed. The swelling data shown in Figure 3 indicates the steadily increased network interaction; the tensile strength of the sample (d) are higher than the sample (c) shown in Table IV. This means the network interaction of the sample (d) is higher than the sample (c). The higher network interaction must confine the movement of rubber chains more efficiently, causing less deformation.

Certain amount of cavitation is another feature shown on higher magnification images in Figure 13 and 14. Cavitation is a common deformation mechanism for hard resin system; it is caused by stress concentration around the added particles or impurities. An amount of particles are visible in Figure 11(c), which might be the additive particles. These particles intend to form cavities in Figure 12(c). Obvious cavities are available for sample (c) and (d), after hours of curing. Both the swelling data in Figure 3 and the mechanical properties in Table IV demonstrate the network interaction increases steadily with prolonging vulcanization. As the rubber chain movement is confined by the increased network interaction, there is a higher hydrostatic tension when a tensile load is applied to specimen, leading to cavitation. Careful observation found that Zone 1 shows higher degree of cavitation than Zone 2; this is caused by the higher stress concentration occurred in Zone 1.

CONCLUSIONS

This research develops the curing mechanism of hard rubber with prolonging vulcanization.

1. In the initial period of curing, polysulfur mainly reacts with SBR macromolecules to form chemical crosslink as evidenced by the significant increase of modulus during vulcanization. The polar combined sulfur modifies the SBR molecules, leading to a large amount of interchain attraction.
2. The swelling analysis shows that most sulfur is reacted with SBR in the first 1–4 h. Both the chemical crosslink and the interchain attraction contribute to the decreased swelling value.
3. While the hardness of SBR depends on chemical crosslink, the Young's modulus relates to the interchain attraction. The tensile strength is mainly dependant on the interchain attraction, rather than the chemical crosslink. The ideal elongation at break for hard rubber can be obtained via at least 4 h of curing. VST improves with vulcanization, showing the contribution of both chemical crosslink and interchain attraction.
4. The thermal stability investigation provides indirect evidence for the proposed curing mechanism. The conversion of hard rubber from soft to hard state is due to the interchain attraction provided by the rubber chains modified by the combined sulfur.
5. The tensile fracture morphology shows transition of fracture characteristics from elastomer to hard resin, supporting the proposed curing mechanisms.

J.M. thanks the Australian Research Council for the award of an Australian Postdoctoral Fellowship, tenable at the University of South Australia.

References

1. Pyne, J. R. Encycl Polym Sci Eng 1988, 14, 670.
2. MacKay, J. R. Mater Methods 1950, 31, 54.
3. Silver, J. R. Trans Am Inst Chem Eng 1927, 19, 71.
4. Barnhart, R. R. Kirk-Othmer Ency. Chem Technol 1968, 17, 587.
5. Meltzer, T. H.; Dermody, W. J. J Appl Polym Sci 1964, 8, 773.
6. Meltzer, T. H.; Dermody, W. J. J Appl Polym Sci 1963, 7, 1493.
7. Meltzer, T. H.; Dermody, W. J. J Appl Polym Sci 1963, 7, 1487.
8. Meltzer, T. H.; Dermody, W. J. J Appl Polym Sci 1965, 9, 3041.
9. Chruch, H. F.; Daynes, H. A. J Rubber Res 1947, 16, 93.
10. Bhaumik, M. L.; Banerjee, D.; Sircar, A. K. J Appl Polym Sci 1962, 4, 366.
11. Bhaumik, M. L.; Banerjee, D.; Sircar, A. K. J Appl Polym Sci 1962, 6, 674.
12. Bhaumik, M. L.; Banerjee, D.; Sircar, A. K. J Appl Polym Sci 1965, 9, 367.
13. Scott, J. R. J Rubber Res 1948, 17, 170.
14. Dermody, W. J Rubber World 1960, 142, 79.
15. Scott, J. R. Ebonite: Its Nature, Properties and Compounding; Maclaren Publications, Inc.: England, London, 1958.
16. Brydson, J. A. Rubbery Materials and Their Compounds; Elsevier Applied Science: London, 1988.
17. Senake Perera, M. C.; Ishiaku, U. S.; Mohd, Z. A. Eur Polym J 2001, 37, 167.
18. Ma, J.; Xu, J.; Zhu, Y. J.; Zhang, L. Q. Polymer 2002, 43, 937.
19. Ismail, H.; Yusof, A. M. M. J Appl Polym Sci 2005, 96, 2181.
20. Daniele, F.; Castro, J. C. M. S., Regina, C. R. N.; Leila, L. Y. V. J Appl Polym Sci 2004, 94, 1575.